Femtosecond Time-Resolved Absorption Spectroscopy of Astaxanthin in Solution and in α-Crustacyanin

Robielyn P. Ilagan,[†] Ronald L. Christensen,[‡] Timothy W. Chapp,[†] George N. Gibson,[§] Torbjörn Pascher,[⊥] Tomáš Polívka,[⊥] and Harry A. Frank*,[†]

Department of Chemistry, University of Connecticut, Storrs, Connecticut 06269-3060, Department of Chemistry, Bowdoin College, Brunswick, Maine 04011-8466, Department of Physics, University of Connecticut, Storrs, Connecticut 06269-3046, and Department of Chemical Physics, Lund University, Box 124, S-22100 Lund, Sweden

Received: December 8, 2004; In Final Form: February 8, 2005

Steady-state absorption and femtosecond time-resolved spectroscopic studies have been carried out on astaxanthin dissolved in CS_2, methanol, and acetonitrile, and in purified α-crustacyanin. The spectra of the $S_0 \rightarrow S_2$ and $S_1 \rightarrow S_n$ transitions were found to be similarly dependent on solvent environment. The dynamics of the excited-state decay processes were analyzed with both single wavelength and global fitting procedures. In solution, the S_1 lifetime of astaxanthin was found to be ∼5 ps and independent of solvent. In α-crustacyanin, the lifetime was noticeably shorter at ∼1.8 ps. Both fitting procedures led to the conclusion that the lifetime of the S_2 state was either comparable to or shorter than the instrument response time. The data support the idea that dimerization of astaxanthin in α-crustacyanin is the primary molecular basis for the bathochromic shift of the $S_0 \rightarrow S_2$ and $S_1 \rightarrow S_n$ transitions. Planarization of the astaxanthin molecule, which leads to a longer effective π-electron conjugated chain and a lower S_1 energy, accounts for the shorter τ_1 in the protein.

Introduction

The species of lobster indigenous to North America, *Homarus americanus*, and its European North Sea relative, *Homarus gammarus*, are most commonly dark brown, but some may appear greenish brown, orange, mottled, or even bright blue (Figure 1). This coloration derives from the presence of the carotenoid, astaxanthin (3,3′-dihydroxy-β,β′-carotene-4,4′-dione; Figure 2),[1] found in the epicuticle, the calcified surface layer of the lobster carapace.[2−4] The variations in coloration are dependent on the extent to which the various forms of astaxanthin—free, aggregated, or bound in the α- and β-crustacyanin carotenoproteins—are expressed by the organism.[5,6] Alterations in color also can be attributed to differences in diet, heredity, environment, and the extent of light exposure.[7] Upon heating, astaxanthin is released from the crustacyanin protein, but remains associated with the crustacean shell, which turns bright red.[6] This remarkable observation is one of the largest reported protein-induced spectral shifts of a bound molecule. The molecular basis of the phenomenon has been the subject of numerous experimental and theoretical investigations.[6,8−15]

The light-absorption properties of astaxanthin and carotenoids are determined primarily by the extent of π-electron conjugation along their C_{40} carbon−carbon bond skeleton.[1] They are further fine-tuned by the presence of functional groups, configurational and conformational twisting, and the polarity and polarizability of the solvent environment.[16] The strong, visible light absorption by carotenoids is known to be due to a $S_0 \rightarrow S_2$ transition (Figure 3).[17,18] The $S_0 \rightarrow S_1$ transition for carotenoids and polyenes is forbidden by symmetry and typically extremely weak.[19−21] Despite numerous detailed spectroscopic investigations of many different carotenoid-containing pigment−protein complexes, the factors controlling the spectral features of protein-bound carotenoids are not well understood.[22−24]

The most distinct carotenoprotein is α-crustacyanin, a member of the diverse, extracellular, ligand-binding, lipocalin family well-known for imparting biological coloration to Crustacea.[5] α-Crustacyanin is formed from five distinct protein subunits denoted A_1, A_2, A_3, C_1, and C_2 which differ in their molecular weights and amino acid compositions.[25,26] These apoproteins are further subdivided into two groups: Type 1, which consists of A_2 and A_3, and Type 2, which consists of A_1, C_1, and C_2.[22] β-Crustacyanin is a dimer of one Type 1 subunit, one Type 2 subunit, and two bound astaxanthin molecules.[22] α-Crustacyanin is a macromolecular complex of 8 β-crustacyanin molecules and contains a total of 16 astaxanthins.[25,26] The recently reported crystal structure of the β-crustacyanin protein at 3.2 Å resolution[27] was formed from subunits A_1 and A_3 interacting in a loop region and displaying the usual β-barrel topology of a lipocalin, which consists of a dimer of discrete β sheets. The two astaxanthin molecules reside in distinct protein environments, crossing the A_1/A_3 subunit interface, with each subunit containing one-half of an astaxanthin. The two astaxanthins come within 7 Å of each other at the central portions of their elongated network of conjugated π-electron carbon−carbon double bonds. The crystal structure shows that the astaxanthins exist in *all-trans* configurations, but are markedly bowed and have their terminal β-ionone rings in the same plane as the chain of the interior π-electron conjugated bonds. α-Crustacyanin has a maximum in its absorption spectrum at ∼630 nm, whereas β-crustacyanin absorbs at ∼590 nm.[28] In solution, astaxanthin has a maximum absorption between 475 and 500 nm, depending on solvent polarizability. The report of the β-crustacyanin

* Address correspondence to this author. Phone: 860-486-2844. Fax: 860-486-6558. E-mail: harry.frank@uconn.edu.
[†] Department of Chemistry, University of Connecticut.
[‡] Department of Chemistry, Bowdoin College.
[§] Department of Physics, University of Connecticut.
[⊥] Department of Chemical Physics, Lund University.

10.1021/jp0444161 CCC: $30.25
Published on Web 03/18/2005

Figure 1. *Homarus americanus* before and after boiling (top) and other color variations (bottom).

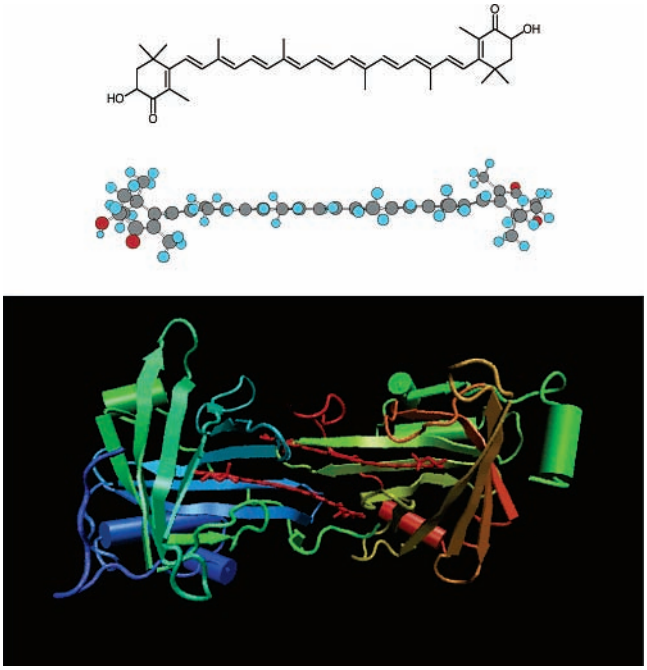

Figure 2. Astaxanthin structure (top), geometry optimized via MOPAC computation using an AM1 Hamiltonian (middle), and in β-crustacyanin based on the PDB data set 1GKA (bottom).

structure by Cianci et al.[27] has spawned several theoretical and experimental investigations to explain the bathochromic shift of the absorption spectrum of the astaxanthin molecule induced upon binding to the crustacyanin protein.

Prior to the report of the β-crustacyanin crystal structure, Weesie et al.[10] used a combination of classical molecular mechanics and a semiempirical quantum chemical model employing an AM1 Hamiltonian to optimize the astaxanthin structure followed by electronic absorption calculations in the gas phase. These computations suggested that the spectral shift observed for astaxanthin in the protein is due to double protonation of the two ring keto groups of astaxanthin (Figure 2).[10] ^{13}C magic angle spinning nuclear magnetic resonance (NMR) and resonance Raman results by the same group were used to support the claim that protonation of the keto groups led to a reduction in the LUMO-HOMO energy gap resulting in a large red shift of the $S_0 \rightarrow S_2$ transition.[8−10] More recently, quantum methods *ab initio* configuration interaction method including only singly excited configurations (CIS), time-dependent density functional theory (TDDFT), and Zerner's intermediate neglect of differential overlap (ZINDO/S) was used to calculate the electronic absorption spectrum of unbound astaxanthin in the gas phase.[11] ZINDO/S predicted the maximum absorption to be 468 nm. This is in good agreement with experimental data of astaxanthin in benzene ($\lambda_{max} = 488$ nm), although the calculations do not account for solvent effects.[11] Semiempirical ZINDO/S computations were also used to evaluate the contributions to the bathochromic shift from various structural perturbations based on the X-ray structure of β-crustacyanin.[11] These computations suggested that the shift is due

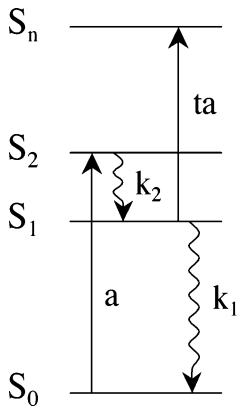

Figure 3. Energy level scheme for astaxanthin. a is absorption and ta is transient absorption. k_1 and k_2 are rate constants associated with the decay of S_1 and S_2, respectively.

mainly to hydrogen bonding of the astaxanthin keto groups to histidine residues and water molecules in the protein. The effect of the histidine was found to be directly dependent on the astaxanthin protonation state.[11] Even more recently, van Wijk et al.[12] used TDDFT calculations on several models based on the X-ray structure of β-crustacyanin to complement their results on ^{13}C NMR and resonance Raman spectroscopy on the ^{13}C-labeled astaxanthins. They postulated that the conformational twisting of astaxanthin induced by protein binding and hydrogen bonding account for only one-third of the total bathochromic shift in α-crustacyanin. They suggested that the spectral properties of α-crustacyanin are determined to a much larger extent by exciton interactions between proximal chromophores.[12] Moreover, the circular dichroism spectrum of β-crustacyanin has been interpreted in terms of exciton splitting between the two twisted astaxanthins.[6,22,28]

In this paper we present ultrafast time-resolved spectroscopic studies of astaxanthin in solution and in α-crustacyanin. This protein complex is one of only a few well-characterized carotenoproteins that do not bind chlorophyll.[24] Thus, the data presented here are important for understanding the intrinsic behavior of carotenoids in a protein environment in the absence of interactions with chlorophyll, which typically would result in excited-state energy transfer between these cofactors. The comparison of the results from α-crustacyanin with those obtained for astaxanthin in solution reveals how the binding of the molecule to the α-crustacyanin protein alters its photophysical behavior. This information is essential for understanding the factors controlling the optical spectroscopy of protein-bound carotenoids.

Materials and Methods

Sample Preparation. Astaxanthin was obtained from Roche and was purified with use of a Millipore Waters 600E high-performance liquid chromatography (HPLC) system equipped with a photodiode array detector. The mobile phase consisted of an isocratic mixture of 11:89 v/v methyl *tert*-butyl ether (MTBE):methanol with a flow rate of 0.5 mL/min on a 3.9 mm × 300 mm Nova Pak C_{18} column. The purified astaxanthin was dried with a gentle stream of nitrogen gas and then redissolved in carbon disulfide (99+% anhydrous), methanol (99.9% A.C.S. spectrophotometric grade), or acetonitrile (99.5+% spectrophotometric grade). All solvents were obtained from Sigma-Aldrich and used without further purification. The α-crustacyanin was obtained as a gift from Dr. George Britton and purified prior to the spectroscopic experiments by applying the sample to a diethylaminoethyl (DEAE)−cellulose column equilibrated with 50 mM potassium phosphate buffer, pH 7. The sample was eluted from the column with 0.1 M KCl in the same buffer.[5]

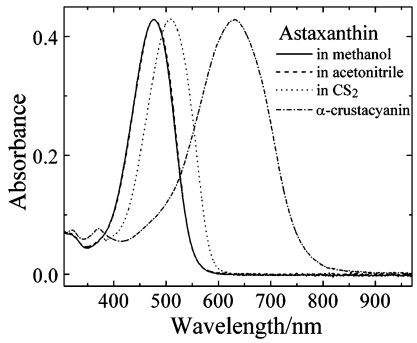

Figure 4. Normalized absorption spectra of astaxanthin in methanol, acetonitrile, CS_2, and α-crustacyanin at room temperature. The spectra in methanol and acetonitrile are essentially superimposable.

Spectroscopy. The optical density of the samples was adjusted to approximately 0.4 at the excitation wavelength in a 2 mm path length cuvette. All transient absorption experiments were carried out at room temperature. The femtosecond transient absorption spectrometer system employs a Spectra-Physics Tsunami mode-locked Ti:sapphire oscillator pumped with a continuous wave, diode-pumped, Nd:YVO4 laser (Millennia, Spectra Physics). The output is amplified by a 1 kHz tunable Spitfire Ti:sapphire regenerative amplifier pumped by an Evolution Nd:YLF pump laser which generates ∼45 fs pulses with an average energy of 800 mJ/pulse at 800 nm. The output beam is passed through a splitter in which most of beam is used to pump the optical parametric oscillator (OPA-800) to generate the excitation wavelength. The OPA-800 produces signal and idler outputs up to 100 μJ and, for the experiments reported here, used a beta-barium borate (BBO) Type I crystal to produce excitation wavelengths from 500 to 600 nm by harmonic generation or sum frequency mixing. The rest of the output beam is used to generate white light continuum probe pulses by using a sapphire plate contained in an Ultrafast System LLC spectrometer. The excitation and probe pulses were overlapped at the sample with their relative polarization set to the magic angle (54.7°). A polarizer was placed before the charge-coupled device (CCD) detector to minimize the scattered signal from the pump pulse. Excitation was 540 nm for astaxanthin in CS_2, 500 nm for astaxanthin in methanol and acetonitrile, and 600 nm for the α-crustacyanin sample. The assignment of time zero was based on the maximum temporal overlap of the pump and the probe pulses. The dynamics showed no dependence on excitation energy from 0.2 to 2.0 μJ/pulse. The sample was stirred with a magnetic microstirrer to avoid sample photodegradation. Absorption spectra of the samples were taken at room temperature to confirm sample integrity before and after the transient absorption experiments. A MatLab program was used to correct for the dispersion in the transient absorption spectra.

Results

Astaxanthin in methanol, acetonitrile, CS_2, and α-crustacyanin displays broad, featureless steady-state absorption spectral line shapes (Figure 4). In methanol and acetonitrile, astaxanthin absorbs at 476 nm, whereas in CS_2 the maximum absorption is at 506 nm. This red-shift can be attributed to the higher polarizability of CS_2, which lowers the $S_0 \rightarrow S_2$ transition energy more than the other solvents. Astaxanthin in α-crustacyanin has an absorption maximum at approximately 630 nm, which accounts for the characteristic blue color of this pigment.

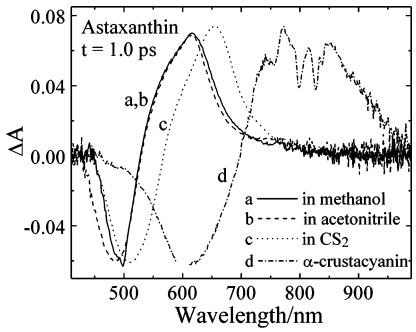

Figure 5. Transient absorption spectra of astaxanthin in methanol, acetonitrile, CS_2, and α-crustacyanin at room temperature taken 1.0 ps after excitation. The excitation wavelength was 540 nm for astaxanthin in CS_2, 500 nm in methanol and acetonitrile, and 600 nm for α-crustacyanin. The spectra were normalized to the amplitude of the ground-state bleaching band that occurs between 450 and 630 nm. The scattering profile of the excitation pulse at 600 nm for α-crustacyanin was removed for clarity. The spectral features in the 750−850 nm region are due to our inability to produce a spectrally flat continuum probe in that region.

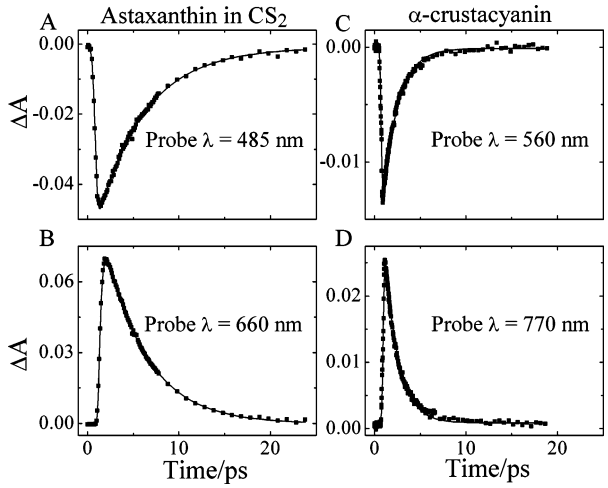

Figure 6. Transient absorption kinetics of astaxanthin in CS_2 excited at 540 nm and of α-crustacyanin excited at 600 nm at room temperature and with 1 μJ energy. (A and C) The bleaching and recovery of the ground-state absorption of astaxanthin in CS_2 probed at 485 nm and of α-crustacyanin probed at 560 nm. (B and D) The rise and decay of the $S_1 \rightarrow S_n$ transient absorption of astaxanthin in CS_2 probed at 660 nm and of α-crustacyanin probed at 770 nm. The solid lines are the fit of the kinetic model (Figure 3, eqs 4−6) to the data.

The transient absorption spectra taken 1.0 ps after excitation for astaxanthin in methanol, acetonitrile, CS_2, and α-crustacyanin are shown in Figure 5. As for the ground-state absorption (Figure 4), a large spectral shift is observed for astaxanthin in α-crustacyanin compared to the molecule in solution. Parts A and C of Figure 6 show the instantaneous bleaching and subsequent recovery of the ground-state absorption that occurs after the excitation pulse for astaxanthin in CS_2 and α-crustacyanin. The recovery of the ground-state absorption in α-crustacyanin (Figure 6C) is faster than that for astaxanthin in CS_2 (Figure 6A). The rise and decay of the $S_1 \rightarrow S_n$ transient absorption (Figure 6B,D) is observed to the red of the signal associated with the bleaching of the ground state. The decay of the transient absorption signal observed for the α-crustacyanin protein also is faster than that observed for astaxanthin in solution (compare part D with part B in Figure 6).

Transient spectra for astaxanthin in CS_2 and α-crustacyanin taken at various time delays are shown in Figures 7A and 8A.

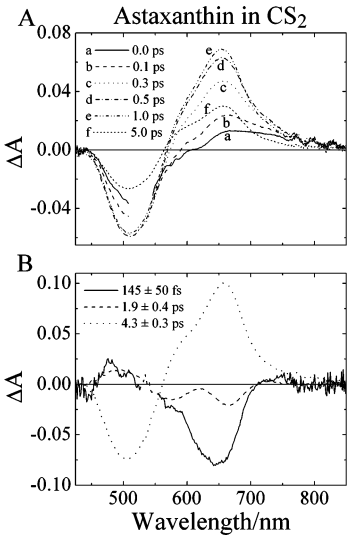

Figure 7. (A) Transient absorption spectra of astaxanthin in CS_2 at different delay times after excitation at 540 nm at room temperature. (B) Spectral profiles of preexponential factors of the decay components obtained from global fitting of astaxanthin in CS_2. See text for details. Sharp spikes at 540 nm arising from the scattered excitation pulse at early times have been removed from profiles a and b in part A and the 145 ± 50 fs trace in part B for clarity.

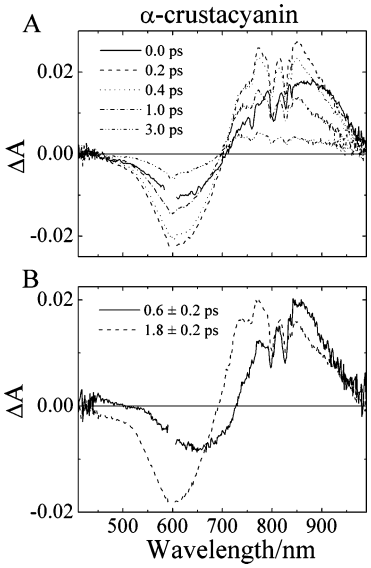

Figure 8. (A) Transient absorption spectra of α-crustacyanin at different delay times after excitation at 600 nm at room temperature. The scattering signal of the excitation pulse at 600 nm was removed for clarity. (B) Spectral profiles of preexponential factors of the decay components obtained from global fitting of astaxanthin in α-crustacyanin. See text for details. The spectral features in the 750−850 nm region are due to our inability to produce a spectrally flat continuum probe in that region.

The spectra shown in Figure 7A are typical of the results from all the solvents. The transient spectra show a broad bleaching in the 450−575 nm region that corresponds to the disappearance of the $S_0 \rightarrow S_2$ absorption band upon excitation. Subsequently, there is a buildup of an excited-state absorption signal in the 575−800 nm region corresponding to an $S_1 \rightarrow S_n$ transition. Virtually identical features are observed for astaxanthin in α-crustacyanin except for the fact that both the bleaching and excited state absorption signals from this sample (Figure 8A) are red-shifted by approximately 100 nm compared to those seen for astaxanthin in CS_2 (Figure 7A).

TABLE 1: S_1 and S_2 Lifetimes, τ_1 and τ_2, of Astaxanthin in Solution and in α-crustacyanin[a]

astaxanthin solvent	pump λ/nm	probe λ[b]/nm	τ_1/ps	τ_2[b]/fs	τ_s/fs	τ_3/ps	fitting procedure
CS_2	540	485	5.3 ± 0.1	n.a.	250 ± 75		single λ
		660	4.6 ± 0.1	320 ± 20	160 ± 40		single λ
		n.a.	4.3 ± 0.3	145 ± 50	210 ± 30	1.9 ± 0.4	global fitting
methanol	500	470	4.9 ± 0.1	n.a.	110 ± 50		single λ
		630	5.0 ± 0.2	80 ± 50	130 ± 40		single λ
		n.a.	5.0 ± 0.3	105 ± 70	110 ± 30		global fitting
acetonitrile	500	470	5.4 ± 0.2	n.a.	150 ± 90		single λ
		630	5.1 ± 0.2	180 ± 70	130 ± 50		single λ
		n.a.	4.9 ± 0.3	165 ± 50	105 ± 50		global fitting
α-crustacyanin	600	560	1.6 ± 0.1	n.a.	100 ± 25		single λ
		770	1.5 ± 0.1	30 ± 15	140 ± 40		single λ
		n.a.	1.8 ± 0.2	<100	130 ± 30	0.6 ± 0.2	global fitting

[a] τ_s is the instrument response time. The τ values were obtained from least-squares analysis of the observed transient spectral responses. For the single wavelength fits, eqs 4−6 were used. For the global fitting eq 7 was used. [b] n.a. = not applicable.

The transient dynamics from all the samples were analyzed by using the kinetic model given in Figure 3. The rate equations are

$$\frac{d[S_0]}{dt} = -\sigma_N I_0 \exp\left(\frac{-t^2}{\tau_s^2}\right) S_0 + k_1 S_1 \quad (1)$$

$$\frac{d[S_2]}{dt} = \sigma_N I_0 \exp\left(\frac{-t^2}{\tau_s^2}\right) S_0 + k_2 S_2 \quad (2)$$

$$\frac{d[S_1]}{dt} = k_2 S_2 - k_1 S_1 \quad (3)$$

where $[S_i]$ is the normalized population of the S_i level, t is time, σ_N is the absorption cross section, τ_s is the instrument response time, I_0 is the peak pump intensity (in photons/cm^2 s), and k_1 and k_2 are decay rate constants for the transitions $S_1 \rightarrow S_0$ and $S_2 \rightarrow S_1$, respectively. The solution to the set of coupled differential equations assumed that the total population in the states, S_0, S_1, and S_2, remained constant over all time and that at negative infinite time, all the population was in the ground state, S_0. The excitation of the molecules via the $S_0 \rightarrow S_2$ transition was assumed to be instantaneous. The percent population decaying directly via $S_2 \rightarrow S_0$ relaxation was assumed to be negligible compared to decay of S_2 via $S_2 \rightarrow S_1$. Integrating eq 1 gives the time dependence of the ground state, S_0, population, which can be used to fit the kinetics of the bleaching of the $S_0 \rightarrow S_2$ transition (Figure 6A,C). The time dependence of the S_1 state population is derived from the coupled set of eqs 1−3 and can be used to fit the $S_1 \rightarrow S_n$ transient absorption dynamics (Figure 6B,D). Approximate analytical solutions to eqs 1, 2, and 3 (where $k_1 \ll k_2$ and $k_1 \ll 1/\tau_s$) are:

$$[S_0] = 1 - \frac{\sqrt{\pi}}{2}\tau_s \sigma_N I_0 \left[1 + \mathrm{erf}\left(\frac{t}{\tau_s}\right)\right] \exp(-k_1 t) \quad (4)$$

$$[S_2] = \frac{\sqrt{\pi}}{2}\tau_s \sigma_N I_0 \left[1 + \mathrm{erf}\left(\frac{t}{\tau_s} - \frac{k_2\tau_s}{2}\right)\right] \exp\left[\left(\frac{k_2\tau_s}{2}\right)^2 - k_2 t\right] \quad (5)$$

$$[S_1] = \frac{\sqrt{\pi}}{2}\tau_s \sigma_N I_0 \left\{\left[1 + \mathrm{erf}\left(\frac{t}{\tau_s}\right)\right] + \exp\left[\left(\frac{k_2\tau_s}{2}\right)^2 - k_2 t\right] \times \left[\mathrm{erf}\left(\frac{k_2\tau_s}{2} - \frac{t}{\tau_s}\right) - 1\right]\right\} \exp(-k_1 t) \quad (6)$$

The S_1 and S_2 lifetimes, τ_1 and τ_2, of astaxanthin in solution and in α-crustacyanin were obtained by fitting these equations to the data. The instrument response time, τ_s, was also treated as a fitting parameter because under the experimental conditions, it is not possible to determine the response function directly with high precision due to the interaction of the pulses with the solvent and the cuvette walls.

To provide deeper insight into the excited-state dynamics of astaxanthin in various environments, a global fitting procedure also was applied for data analysis.[29] All 512 kinetics traces recorded for each experiment were fitted simultaneously by using a multiexponential function

$$S(\lambda,t) = \sum_i A_i(\lambda) \exp(-\tau_i/t) \quad (7)$$

where τ_i and A_i are the time constant and preexponential factors of decay component i. Because a particular excited-state decay must have the same time constant regardless of the probing wavelength, this approach provides better information about the excited-state dynamics than single-trace fitting. The quality of the global fits and the number of decay components necessary to reproduce the experimental data were evaluated by minimization of χ^2 and a flatness of the residual matrix, an array containing residuals of all 512 decays.

The single wavelength and global fitting procedures converged on a value of ∼5 ps for τ_1, the S_1 lifetime of astaxanthin in all solvents. However, in α-crustacyanin, τ_1 was noticeably shorter at ∼1.8 ps. Both fitting procedures led to the conclusion that the lifetime of the S_2 state was either comparable to or shorter than the instrument response time except possibly for astaxanthin in CS_2. The S_1 and S_2 dynamics are summarized in Table 1.

Discussion

Intramolecular relaxation of the photoexcited S_1 and S_2 states of carotenoids proceeds primarily via nonradiative pathways. For astaxanthin in methanol and in acetonitrile, the dynamics obtained from single wavelength fitting and from global analysis are in good agreement (Table 1). In these cases, two kinetic components, k_1 and k_2 (Figure 3), corresponding to time constants, $\tau_1 \approx 5$ ps and $\tau_2 \approx 100-200$ fs ($\tau_i = 1/k_i$) were sufficient to account for the kinetic behavior (Table 1). While the single wavelength fits at 485 and 660 nm could individually model astaxanthin in CS_2, the fits were not self-consistent. This is seen in the fact that the two values of τ_1 and of τ_s obtained from the single wavelength fits lie outside the range spanned by their respective uncertainties (Table 1). This is not the case in the other experiments. For astaxanthin in CS_2, this implies that the model in Figure 3 is not sufficient to explain the data. However, for this system, the solution by global fitting was

improved by adding a third decay component. The time constants obtained for these experiments were $\tau_1 = 4.3 \pm 0.3$ ps, $\tau_2 = 145 \pm 50$ fs, and $\tau_3 = 1.9 \pm 0.4$ ps. The amplitude spectra constructed from the wavelength dependence of the preexponential factors, $A_i(\lambda)$ (eq 7), of these components are shown in Figure 7B. The negative values of the 145 fs component in the spectral region of the $S_1 \rightarrow S_n$ band (550 to 750 nm) indicate that this component is due to a rise of the $S_1 \rightarrow S_n$ band and thus can associated with $S_2 \rightarrow S_1$ relaxation. The 4.3 ps component is associated with the decay of the $S_1 \rightarrow S_n$ band and the recovery of the ground-state bleaching (Figure 4) and corresponds to the S_1 lifetime. On the other hand, the spectral profile of the 1.9 ps component suggests that it has its origin in a blue-shift of the $S_1 \rightarrow S_n$ band because it decays on the red side of the $S_1 \rightarrow S_n$ band, while a negative value on the blue side of this band indicates a 1.9 ps rise in this spectral region. In addition, the larger negative amplitude of this component at 560 nm suggests that it is connected with a formation of the shoulder located at 560 nm, which is clearly visible in the transient absorption spectra at later delay times (e.g. spectrum f in Figure 7A). Such behavior is consistent with equilibration in the S_1 state, but the origin of this process is not easy to discern. It does not seem to be due to S_1 vibrational relaxation, for which a large blue shift and narrowing is observed.[30,31] The behavior of the 1.9 ps component is reminiscent of that observed for peridinin, which was ascribed to equilibration between the S_1 and ICT states.[32] However, since no stabilization of the ICT state is observed for astaxanthin (see below), such an assignment can be ruled out. Other processes, such as involvement of a so-called S* state, usually exhibited as a blue shoulder at the $S_1 \rightarrow S_n$ band,[33] or excited-state solvation, which has a characteristic time constant of ~2 ps for CS_2,[34] cannot be ruled out. We thus cannot unequivocally assign the 1.9 ps component to a particular process. However, it makes only a minor contribution to the excited-state dynamics, representing less than 10% of the total amplitude at any wavelength.

Similar to astaxanthin in CS_2, the dynamics of astaxanthin in α-crustacyanin analyzed by global fitting required three decay components. The fastest component has a time constant of <100 fs, comparable to the time resolution of the instrument, and can be associated with the time constant for the decay of S_2 to S_1. The other two components decay in 1.8 and 0.6 ps, and their spectral profiles are shown in Figure 8B. The profile of the 1.8 ps component is consistent with $S_1 \rightarrow S_n$ absorption and confirms that the S_1 lifetime of astaxanthin in α-crustacyanin is shorter than that in solution (Table 1). The 0.6 ps component is exhibited as a decay in the 750−950 nm spectral region and becomes dominant above 840 nm. The behavior of this component is thus markedly different from that of the 1.9 ps component found for astaxanthin in CS_2. The spectral profile of the 0.6 ps component is consistent with vibrational relaxation in the S_1 state.[30,31] The remaining question is why the S_1 vibrational relaxation is pronounced only for astaxanthin bound to α-crustacyanin. This could be related to the fact that astaxanthin in the protein is significantly bowed, and its β-ionone rings are more planar than in solution. This strained, thermodynamically unstable conformation of the protein-bound astaxanthin could lead to shifts in the S_1 and S_2 potential energy surfaces promoting formation of vibrationally hot S_1 states in α-crustacyanin. It is also possible that the S_1 vibrational relaxation for astaxanthin in solution occurs on time scales comparable to $S_2 \rightarrow S_1$ relaxation, thus population of the vibrationally hot S_1 state in solution is very low, preventing its observation. The planar conformation of astaxanthin in the protein (described above) may result in slower S_1 vibrational relaxation, as observed for zeaxanthin bound to a carotenoprotein from human retina.[35]

The S_1 lifetime of astaxanthin is essentially unaffected by solvent (Table 1). Yet, many carbonyl-containing carotenoids exhibit a shortening of the S_1 lifetime with increasing solvent polarity.[36−38] This has been interpreted in terms of the presence of an intermolecular charge transfer (ICT) state coupled to S_1 that is stabilized in polar solvents and leads to faster rates of decay in those media.[24,36−38] This effect is not seen for astaxanthin, supporting recent hypotheses that orientation and position of the carbonyl group with respect to the conjugated backbone is a decisive factor for polarity-induced effects.[37−39] For long carotenoids having the carbonyl group at the end of the conjugated backbone in an *s-cis* orientation with respect to the rest of the conjugation (e.g. spheroidenone), no polarity-induced change of the S_1 lifetime was observed.[37,38] Similarly, the S_1 lifetime is independent of solvent polarity for the long carbonyl carotenoid hydroxyechinenone, which, like astaxanthin, has its carbonyl group in the β-ionone ring.[39] For both spheroidenone and hydroxyechinenone, however, other polarity-induced effects such as weak additional bands in their transient absorption spectra were observed.[37−39] No such effects are seen for astaxanthin (Figure 5), suggesting that the extension of the conjugation and the carbonyl group to both terminal rings prevents the polarity-induced behavior.

The S_1 dynamics of carotenoids also are sensitive to the extent of π-electron conjugation.[40] The energy gap law for radiationless transitions set forth by Englman and Jortner[41] appears to be valid in its weak coupling limit for describing the relationship between the $S_1 \rightarrow S_0$ energy difference and the rate of $S_1 \rightarrow S_0$ radiationless decay (k_1) in carotenoids.[42] The more planar terminal β-ionone rings for astaxanthin in the protein compared to solution should result in a longer effective π-electron conjugation length for the molecule in the protein complex. This should lead to a lower S_1 energy and, consequently, a shorter S_1 lifetime. In solution, astaxanthin adopts a conformation in which the nine interior carbon−carbon double bonds form an extended, approximately planar chain. The remaining carbon−carbon and carbonyl bonds in the terminal rings are in an *s-cis* orientation with respect to the linear chain, and nonbonded interactions force these bonds out of plane with respect to the plane of conjugation of the interior π-electron system (Figure 2). The crystal structure of canthaxanthin,[43] which lacks the hydroxy groups of astaxanthin but is otherwise identical, indicates that the two planes of conjugation in the rings form ~43° dihedral angles with the interior plane of conjugation, significantly reducing the effective conjugation length of what is formally a molecule with 13 conjugated bonds ($N = 13$). The reduction in effective conjugation length (N_{eff}) is manifested in significant blue shifts in the strongly allowed $S_0 \rightarrow S_2$ absorption in carotenoids possessing terminal β-ionone rings, e.g., β-carotene ($\lambda = 477$ nm (hexane)), versus comparable molecules without these steric restrictions, e.g., lycopene ($\lambda = 504$ nm (hexane)). The lack of planarity between the double bonds in the ring and those along the interior polyene chain undoubtedly leads to an increase in the S_1 energy and a systematic increase in the S_1 lifetime. The flattening of the astaxanthin molecule in the protein thus should restore the effective conjugation length to $N_{\text{eff}} \approx 13$. This simple picture explains the good agreement between the S_1 lifetime of astaxanthin in α-crustacyanin (~1.8 ps) and the S_1 lifetime of spirilloxanthin (1.4 ps),[44] an open-chain, nonsterically hindered carotenoid with $N = 13$. The energy-gap law also suggests that

astaxanthin in α-crustacyanin and spirilloxanthin in solution must have comparable S_1 energies (~11 500 cm^{-1}).[45] The increase in the S_1 lifetime for astaxanthin in solution (~5 ps) is consistent with a carotenoid having $N_{eff} \approx 11$, cf. the 3.8 ps S_1 lifetime in lycopene.[44] We thus conclude that the loss of steric-induced twisting of the β-ionone rings in astaxanthin upon binding to the α-crustacyanin protein leads to increased planarity of the conjugated system in the protein binding site. Lengthening of the effective conjugation length is the primary reason for the shortening of the lifetime of astaxanthin in α-crustacyanin relative to its value in solution.

The results from these time-resolved experiments are consistent with the extension of the effective polyene conjugation length due to planarization of the astaxanthin molecules in α-crustacyanin. Exciton interactions are not expected to be important in modulating the energy of the $S_0 \leftrightarrow S_1$ transition owing to its forbidden nature. However, exciton couplings in α-crustacyanin have been suggested to play a dominant role in the large bathochromic shift of the $S_0 \rightarrow S_2$ transition.[12] The parallel large red-shift in the strongly allowed $S_1 \rightarrow S_n$ transition reported here supports the notion of strong exciton coupling between the proximal astaxanthins. The $S_0 \rightarrow S_2$ and $S_1 \rightarrow S_n$ transitions both originate from states having A_g^- symmetry and, as evidenced by the strength of the transitions, terminate in states of B_u^+ symmetry.[24] In α-crustacyanin these transitions are substantially red-shifted from what would be expected for a planar, $N = 13$ carotenoid such as spirilloxanthin, which exhibits an $S_0 \rightarrow S_2$ (0−0) transition at 525 nm and a strong $S_1 \rightarrow S_n$ transient absorption at ~590 nm in *n*-hexane.[33] To get an idea of a characteristic protein-induced change in absorption, both of these values are shifted only 30 nm to the red in the photosynthetic bacterial LH1 antenna pigment−protein complex.[33] In α-crustacyanin the $S_0 \rightarrow S_2$ transition appears at ~630 nm (Figure 4) and the $S_1 \rightarrow S_n$ transition appears at ~800 nm (Figure 5d). Comparing these values to those from the planar, $N = 13$, spirilloxanthin molecule, a change of the $S_0 \rightarrow S_2$ transition from 525 to ~630 nm corresponds to a 3200 cm^{-1} difference in energy. This is comparable to that seen for the $S_1 \rightarrow S_n$ transition, which changes from ~590 nm for spirilloxanthin in *n*-hexane to ~800 nm in α-crustacyanin and amounts to a 3600 cm^{-1} energy shift. These bathochromic shifts are consistent with the TDDFT computations carried out by van Wijk et al.,[12] who used the coordinates of β-crustacyanin[27] to obtain an exciton splitting of ~4000 cm^{-1} for the $S_0 \rightarrow S_2$ transition.

We conclude that dimerization of astaxanthin in α-crustacyanin accounts for the major portion of the bathochromic shift of both the $S_0 \rightarrow S_2$ and $S_1 \rightarrow S_n$ transitions while planarization of astaxanthin leads to a longer effective π-electron conjugated chain, a lower S_1 energy, and consequently a shorter τ_1 in the protein compared to that in solution.

Acknowledgment. This research is supported in the laboratory of H.A.F. by the National Institutes of Health (GM-30353), the National Science Foundation (MCB-0314380), and the University of Connecticut Research Foundation. The ultrafast laser system was purchased with an NSF MRI grant (CHE-0320403) awarded to G.N.G. and H.A.F. Funding for T.W.C. was provided by an NSF Research Experience for Undergraduates (REU) program (CHE-0354012) at the University of Connecticut. R.L.C. is supported by the Bowdoin College Kenan and Porter Fellowship Programs and also acknowledges the donors of the Petroleum Research Fund, administered by the American Chemical Society, for support of this research. T.P. thanks the Swedish Energy Agency for financial support.

References and Notes

(1) *Carotenoids*; Isler, O., Ed.; Birkhauser: Basel, Switzerland, 1971.
(2) Wald, G.; Nathanson, N.; Jencks, W. P.; Tarr, E. *Biol. Bull., Woods Hole* **1948**, *95*, 249.
(3) Cheesman, D. F.; Zagalsky, P. F.; Ceccaldi, H. J. *Proc. R. Soc. London Ser. B* **1966**, *164*, 130.
(4) Zagalsky, P. F.; Cheesman, D. F. *Biochem. J.* **1963**, *89*, 21P.
(5) Zagalsky, P. F. Invertebrate Carotenoproteins. In *Methods in Enzymology*; Academic Press: New York, 1985; Vol. III, p 216.
(6) Britton, G.; Weesie, R. J.; Askin, D.; Warburton, J. D.; Gallardo-Guerrero, L.; Jansen, F. J.; de Groot, H. J. M.; Lugtenburg, J.; Cornard, J.-P.; Merlin, J.-C. *Pure Appl. Chem.* **1997**, *69*, 2075.
(7) Factor, J. R.; Clemetson, A. Life as a Lobster in Long Island Sound: Biology and Life Cycle. In *Lobster Health News Supplement*, 2003, published by the Sea Grant College Programs of Connecticut and New York.
(8) Weesie, R. J.; Jansen, F. J. H. M.; Merlin, J. C.; Lugtenburg, J.; Britton, G.; de Groot, H. J. M. *Biochemistry* **1997**, *36*, 7288.
(9) Weesie, R. J.; Verel, R.; Jansen, F. J. H. M.; Britton, G.; Lugtenburg, J.; de Groot, H. J. M. *Pure Appl. Chem.* **1997**, *69*, 2085.
(10) Weesie, R. J.; Merlin, J. C.; De Groot, H. J. M.; Britton, G.; Lugtenberg, J.; Jansen, F. J.; Cornard, J. P. *Biospectroscopy* **1999**, *5*, 358.
(11) Durbeej, B.; Eriksson, L. A. *Chem. Phys. Lett.* **2003**, *375*, 30.
(12) van Wijk, A. A. C.; Spaans, A.; Uzunbajakava, N.; Otto, C.; M., d. G. H. J.; Lugtenburg, J.; Buda, F. *J. Am. Chem. Soc.* **2005**, *127*, 1438.
(13) Dellisanti, C. D.; Spinelli, S.; Cambillau, C.; Findlay, J. B. C.; Zagalsky, P. F.; Finet, S.; Receveur-Brechot, V. *FEBS Lett.* **2003**, *544*, 189.
(14) Hoischen, D.; Colmenares, L. U.; Liu, J.; Simmons, C. J.; Britton, G.; Liu, R. S. H. *Bioorg. Chem.* **1998**, *26*, 365.
(15) Krawczyk, S.; Britton, G. *Biochim. Biophys. Acta* **2001**, *1544*, 301.
(16) *The Photochemistry of Carotenoids*; Frank, H. A., Young, A. J., Britton, G., Cogdell, R. J., Eds.; Kluwer Academic Publishers: Dordrecht, The Netherlands, 1999; Vol. 8.
(17) Cogdell, R. J.; Frank, H. A. *Biochim. Biophys. Acta* **1987**, *895*, 63.
(18) Christensen, R. L. The electronic states of carotenoids. In *The Photochemistry of Carotenoids*; Frank, H. A., Young, A. J., Britton, G., Cogdell, R. J., Eds.; Kluwer Academic Publishers: Dordrecht, The Netherlands, 1999; Vol. 8, p 137.
(19) Hudson, B. S.; Kohler, B. E. *J. Chem. Phys.* **1973**, *59*, 4984.
(20) Hudson, B.; Kohler, B. *Annu. Rev. Phys. Chem.* **1974**, *25*, 437.
(21) Hudson, B. S.; Kohler, B. E.; Schulten, K. Linear polyene electronic structure and potential surfaces. In *Excited States*; Lim, E. D., Ed.; Academic Press: New York, 1982; Vol. 6, p 1.
(22) Chayen, N. E.; Cianci, M.; Grossman, J. G.; Habash, J.; Helliwell, J. R.; Nneji, G. A.; Raftery, J.; Rizkallah, P. J.; Zagalsky, P. F. *Acta Crystallogr. D* **2003**, *59*, 2072.
(23) Zagalsky, P. F. *Acta Crystallogr. D* **2003**, *D59*, 1529.
(24) Polívka, T.; Sundström, V. *Chem. Rev.* **2004**, *104*, 2021.
(25) Britton, G.; Armitt, G. M.; Lau, S. Y. M.; Patel, A. K.; Shone, C. C. In *Carotenoid Chemistry and Biochemistry*; Britton, G., Goodwin, T. W., Eds.; Pergamon Press: Oxford, UK, 1982; p 237.
(26) Zagalsky, P. F. In *Carotenoids*; Britton, G., Liaaen-Jensen, S., Pfander, H., Eds.; Birkhauser: Basel, Switzerlands, 1995; Vol. 1A, p 287.
(27) Cianci, M.; Rizkallah, P. J.; Olczak, A.; Raftery, J.; Chayen, N. E.; Zagalsky, P. F.; Helliwell, J. R. *Proc. Natl. Acad. Sci. U.S.A.* **2002**, *99*, 9795.
(28) Buchwald, M.; Jencks, W. P. *Biochemistry* **1968**, *7*, 844.
(29) van Stokkum, I. H. M.; Larsen, D. S.; van Grondelle, R. *Biochim. Biophys. Acta* **2004**, *1657*, 82.
(30) Billsten, H. H.; Zigmantas, D.; Sundstrom, V.; Polivka, T. *Chem. Phys. Lett.* **2002**, *355*, 465.
(31) de Weerd, F. L.; van Stokkum, I. H. M.; van Grondelle, R. *Chem. Phys. Lett.* **2002**, *354*, 38.
(32) Papagiannakis, E.; Larsen, D. S.; van Stokkum, I. H. M.; Vengris, M.; Hiller, R. G.; van Grondelle, R. *Biochemistry* **2004**, *43*, *15303*.
(33) Gradinaru, C. C.; Kennis, J. T. M.; Papagiannakis, E.; van Stokkum, I. H. M.; Cogdell, R. J.; Fleming, G. R.; Niederman, R. A.; van Grondelle, R. *Proc. Natl. Acad. Sci. U.S.A.* **2001**, *98*, 2364.
(34) Horng, M. L.; Gardecki, J. A.; Papazyan, A.; Maroncell, M. *J. Phys. Chem.* **1995**, *99*, 17311.
(35) Billsten, H. H.; Bhosale, P.; Yemelyanov, A.; Bernstein, P. S.; Polivka, T. *Photochem. Photobiol.* **2003**, *78*, 138.
(36) Bautista, J. A.; Connors, R. E.; Raju, B. B.; Hiller, R. G.; Sharples, F. P.; Gosztola, D.; Wasielewski, M. R.; Frank, H. A. *J. Phys. Chem. B* **1999**, *103*, 8751.
(37) Frank, H. A.; Bautista, J. A.; Josue, J.; Pendon, Z.; Hiller, R. G.; Sharples, F. P.; Gosztola, D.; Wasielewski, M. R. *J. Phys. Chem. B* **2000**, *104*, 4569.

(38) Zigmantas, D.; Hiller, R. G.; Sharples, F. P.; Frank, H. A.; Sundstrom, V.; Polivka, T. *Phys. Chem. Chem. Phys.* **2004**, *6*, 3009.
(39) Polivka, T.; Kerfeld, C. A.; Pascher, T.; Sundstrom, V. *Biochemistry* **2005**, *44*, 3994.
(40) Frank, H. A.; Desamero, R. Z. B.; Chynwat, V.; Gebhard, R.; van der Hoef, I.; Jansen, F. J.; Lugtenburg, J.; Gosztola, D.; Wasielewski, M. R. *J. Phys. Chem. A* **1997**, *101*, 149.
(41) Englman, R.; Jortner, J. *Mol. Phys.* **1970**, *18*, 145.
(42) Chynwat, V.; Frank, H. A. *Chem. Phys.* **1995**, *194*, 237.
(43) Bart, J. C. J.; MacGillavry, C. H. *Acta Crystallogr. B* **1968**, *24*, 1587.
(44) Frank, H. A.; Chynwat, V.; Desamero, R. Z. B.; Farhoosh, R.; Erickson, J.; Bautista, J. *Pure Appl. Chem.* **1997**, *69*, 2117.
(45) Papagiannakis, E.; van Stokkum, I. H. M.; van Grondelle, R.; Niederman, R. A.; Zigmantas, D.; Sundstrom, V.; Polivka, T. *J. Phys. Chem. B* **2003**, *107*, 11216.